GEOLOGY OF TERRESTRIAL PLANETS WITH DYNAMIC ATMOSPHERES

RONALD GREELEY
Department of Geology
Box 871404
Arizona State University
Tempe, AZ 85287-1404
Phone: (602) 965-7045
Fax: (602) 965-8102
E-mail: Greeley@asu.edu

ABSTRACT

Geological exploration of the solar system shows that solid-surfaced planets and satellites are subject to endogenic processes (volcanism and tectonism) and exogenic processes (impact cratering and gradation). The present appearance of planetary surfaces is the result of the complex interplay of these processes and is linked to the evolution of planets and their environments. Terrestrial planets that have dynamic atmospheres are Earth, Mars, and Venus. Atmospheric interaction with the surfaces of these planets, or *aeolian activity*, is a form of gradation. The manifestation of aeolian activity is the weathering and erosion of rocks into sediments, transportation of the weathered debris (mostly sand and dust) by the wind, and deposition of windblown material. Wind-eroded features include small-scale ventifacts (wind-sculptured rocks) and large-scale landforms such as yardangs. Wind depositional features include dunes, drifts, and mantles of windblown sediments. These and other aeolian features are observed on Earth, Mars, and Venus.

1. Introduction

Planetary surfaces are shaped or modified by various geological processes, including volcanism, tectonism, and impact cratering. Terrestrial planets that have dynamic atmospheres are further modified by agents of weathering, erosion, transportation, and deposition. For example, depending on past and present atmospheric environments, water and other fluids play an important role in surface modification of some planets. Running water is clearly important on Earth and appears to have been important in the past on Mars (Fig. 1).

In this brief review, attention is focused on processes associated with wind, or *aeolian activity*. Earth, Mars, and Venus all currently experience aeolian activity, and probably have been modified by wind throughout much of their geologic history. These planets afford the opportunity to study a basic geological process--aeolian activity--in a comparative sense, with each planet being a vast natural laboratory having strikingly different environments (Table 1). Because terrestrial aeolian processes and features

Earth, Moon, and Planets **67**: 13–29, 1995.

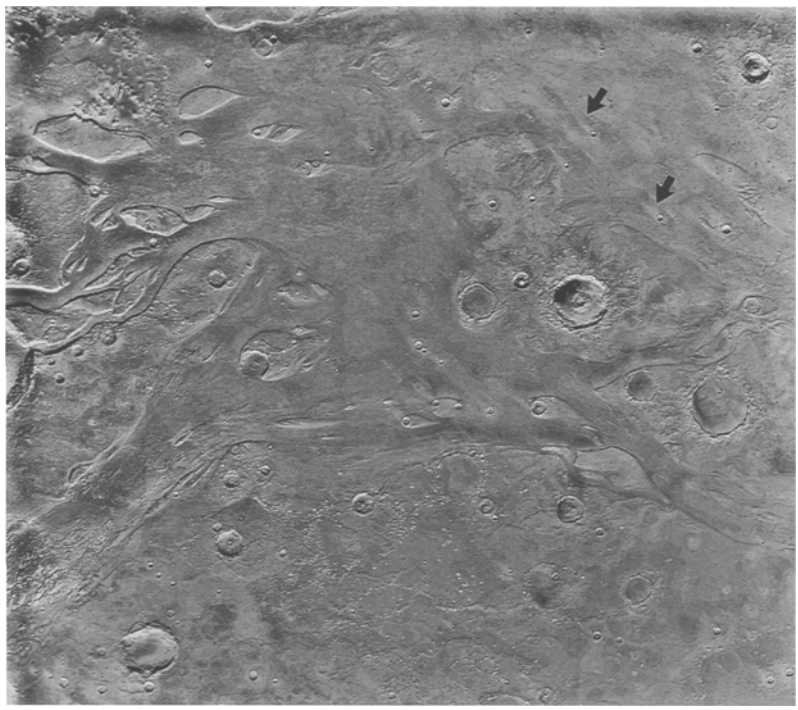

Fig. 1:
Viking Orbiter mosaic of Mars showing terrain modified by channels presumably eroded by water at a time when liquid water could exist on the surface. Also visible (arrows) are wind streaks, which are albedo patterns formed by the wind. Area shown is about 730 km by 850 km where Ares Vallis and Tiu Vallis debouch to the north (top) into Chryse Planitia. Region in the middle of the mosaic on the channel deposits has been selected as the nominal Mars Pathfinder landing site. Images in the mosaic were taken under morning illumination (sun is shining from right to left) (Viking Orbiter mosaic ASU IPF-873, centered at 20°N, 33°W).

have been studied for many years, Earth is the primary planet for comparison with Venus and Mars. However, because surface processes are much more complicated on Earth (primarily because of the presence of liquid water and vegetation) many aspects of aeolian processes that are difficult to assess on Earth are better studied on other planets.

Aeolian processes are capable of redistributing enormous quantities of sediment over planetary surfaces, resulting in the formation of landforms large enough to be seen from orbit and deposition of windblown sediments that can be hundreds of meters thick and cover thousands of square kilometers. Any process capable of effecting these

TABLE 1. Relevant properties of terrestrial planets subject to aeolian processes

	Venus	Earth	Mars
Mass (Earth = 1)	0.814	1	0.108
Density (water =1)	5.25	5.52	3.94
Surface gravity (cm s^{-2})	903	981	373
Atmosphere (main components)	CO_2	N_2,O_2	CO_2
Atmospheric pressure at surface (millibars)	9×10^4	10^3	7.5
Mean temperature at surface (°C)	480°	22°	-23°

changes is relevant to understanding the geological environment of the planets so involved. Furthermore, because aeolian processes involve the interaction of the atmosphere and lithosphere, an understanding of aeolian activity sheds light on meteorological problems.

The study of planetary aeolian processes requires a multidisciplinary, multi-task approach. Consequently, teams of geologists, engineers, and atmospheric scientists often approach aeolian research through the following tasks:

- Use spacecraft data and observations to identify the general problem and isolate specific factors for study (e.g., determine the minimum wind speeds that are required to entrain particles in different planetary environments).
- Conduct laboratory simulations for the 'Earth case' in which various parameters can be controlled (e.g., wind tunnel tests of particle threshold).
- Carry out field work to test the laboratory results under natural conditions to verify that the simulations were done correctly (e.g., observe and measure particle threshold in the field).
- Carry out laboratory experiments for the extraterrestrial cases, duplicating or simulating as nearly as possible the planetary environment involved (e.g., particle threshold tests under martian and venusian atmospheric conditions).
- Extrapolate the results to the planetary case using the laboratory results and theory (for parameters that cannot be duplicated, such as reduced gravity for Mars).

This approach not only provides a logical means for solving extraterrestrial problems, but also contributes toward a better understanding of aeolian processes on Earth.

2. Aeolian processes

Any planet that has a dynamic atmosphere with winds above a critical speed and a surface with small, loose particles has the potential for aeolian activity (Greeley and Iversen, 1985). Winds moving across a surface possess energy and can accomplish geologic work, primarily in the form of removing and transporting sand and dust. The stronger the wind, the greater the effect. The physics of windblown particles are eloquently given in the classic book by Bagnold (1941). Wind transports sediments in three modes: *suspension* (mostly silt and clay particles, i.e., smaller than about 60 μm), *saltation* (a hopping mode involving mostly sand size particles, 60 to 200 μm in diameter), and *surface creep* (particles larger than about 200 μm in diameter). Particles of these sizes can be generated on planetary surfaces from a wide variety of processes, including chemical and physical weathering, impact cratering, volcanic explosions, and tectonic deformation.

Wind threshold curves (Fig. 2) define the minimum wind speeds required to initiate movement of different sizes of particles for given planetary environments (Iversen et al., 1976a). The ability of wind to attain threshold speed is a function primarily of atmospheric density. Thus, the very low density atmosphere on Mars (the surface pressure is about 1/200 that of Earth) requires wind speeds that are about an order of magnitude stronger than on Earth. Conversely, in the very dense venusian atmosphere, very low wind speeds can set particles into motion. The density effect can be considered partly in terms of the number of gas molecules impinging on and passing over the particles to be moved; for the same amount of work to be done in the low density martian atmosphere (fewer molecules) the wind must be moving faster to achieve the same effective flux of molecules. Although this is an oversimplification, it

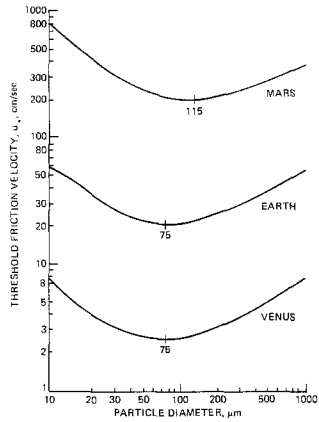

Fig. 2:
Wind threshold curves for particles of different sizes on Earth, Mars, and Venus (from Iversen et al., 1976a).

demonstrates to a first order the relationship between atmospheric density and wind velocity for particle entrainment.

As Fig. 2 shows, regardless of planet the sizes of particles most easily moved (lowest wind friction velocities) are 80 to 100 μm in diameter, or fine sand. Finer particles such as dust become increasingly difficult to set into motion under most circumstances. This results from at least two factors. First, very small grains are immersed in a laminar sublayer beneath the boundary layer and hence the wind is less effective in dislodging the grains. Second, various interparticle forces, such as cohesion and electrostatic charges (surface effects), become more pronounced with decreasing particle diameter because the surface area-to-mass ratio increases, enhancing the surface forces of attraction (Iversen et al., 1976b).

Recent laboratory experiments under martian conditions, however, demonstrate that dust settled on small (~cm) rocks can be entrained about as easily as fine sand (Greeley et al., 1994a). The rocks induce local turbulence and dust settled on the tops of rocks is placed in the turbulent boundary layer. Thus, the geologic setting and the characteristics of the surface are additional considerations of the aeolian environment.

3. Mars

Wind processes in the form of dust storms were suspected to occur on Mars even before Mariner 9 returned conclusive evidence of aeolian activity in 1971. Earthbased observations made over the last 100 years showed albedo patterns that were attributed to a variety of processes, including dust storms, as reviewed by Kahn et al. (1992), Zurek et al. (1992), and Martin and Zurek (1993). Early predictions of the wind velocities required to set particles in motion were based on knowledge of the composition and density of the martian atmosphere (Sagan and Pollack, 1969). Wind tunnel tests conducted under low atmospheric pressure in a martian simulation substantiated these estimates (Greeley et al., 1976, 1977, 1980).

Mariner 9 and the Soviet spacecraft Mars 2 and 3 arrived at Mars in 1971 during a major global dust storm, amply verifying the speculations and predictions of martian aeolian processes. After the dust cleared, the Mariner 9 cameras revealed abundant

Fig. 3:
Viking Orbiter image shows small dust clouds (arrows) rising from lava flow surfaces in the southern Tharsis region of Mars (from Briggs et al., 1977); area shown is 65 km by 80 km (Viking Orbiter image 56A64).

features attributed to aeolian activity, including dunes, wind-eroded hills (yardangs), and various pits and grooves considered to be wind deflation features (McCauley, 1973). The Viking mission (1976-1981) added substantially to the catalog of martian aeolian features and provided details not previously observed (Thomas and Gierasch, 1985; Fig. 3), including the first lander images from the surface of Mars which showed fine-grained material described as aeolian drift deposits (Arvidson et al., 1978). By far, the most abundant aeolian features are wind streaks and other albedo patterns that change size, shape, and position in response to winds.

Reviews of aeolian features and processes on Mars are given by Lee et al. (1982), Thomas et al. (1981), Greeley and Iversen (1985), Greeley et al (1992), and others. Dust deposits are discussed by Christensen (1986, 1988) and others, and reviewed by Christensen and Moore (1992).

3.1. DUNES

Dunes were discovered on Mars on Mariner 9 images (Sagan et al., 1972; Cutts and Smith, 1973). Because dunes are composed of grains that saltate, and because sand is the size grain typically moved in saltation (regardless of planetary environment), it is assumed that the martian dunes (Fig. 4) are composed of grains 60 to 2000-μm in diameter (i.e., "sand").

The Viking mission provided a wealth of information on martian dunes and dune forms. One of the most striking discoveries was the huge sand sea of the north polar region. The field covers more than 7×10^5 km^2, larger than Rub Al Khali in Arabia, the

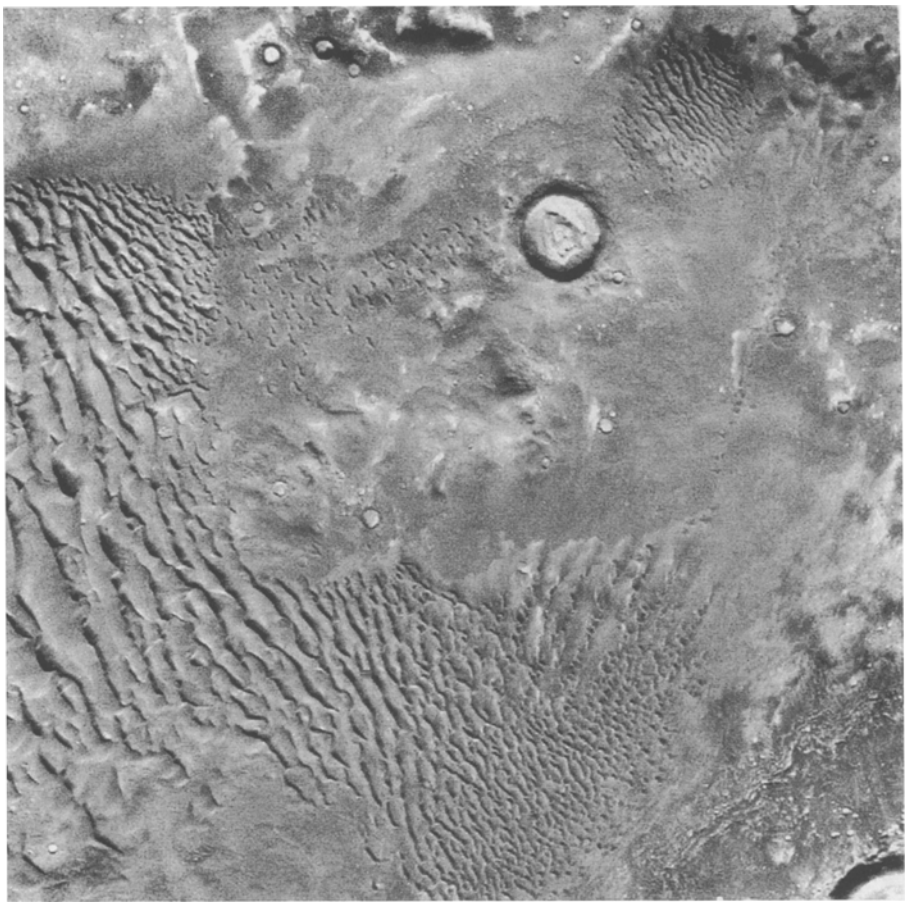

Fig. 4:
Sand dune fields on the floor of the martian crater Kaiser showing transverse dunes of a large (upper part of picture) and small (lower right) field and individual barchan dunes (above the crater). From the shape of the dunes, the prevailing wind direction at the time of dune formation was from the top of the image to the bottom; area shown is about 52 km by 52 km (Viking Orbiter image 575B60).

largest active erg on Earth. All of the martian north polar dunes are either transverse or barchan forms (Fig. 5). Mapping the dune morphologies (Tsoar et al., 1979; Breed et al., 1979) and other indicators of wind directions have enabled maps of the wind circulation pattern for the north polar area to be derived. Two major wind directions are suggested, off-pole winds that become easterly due to coriolis forces during summer,

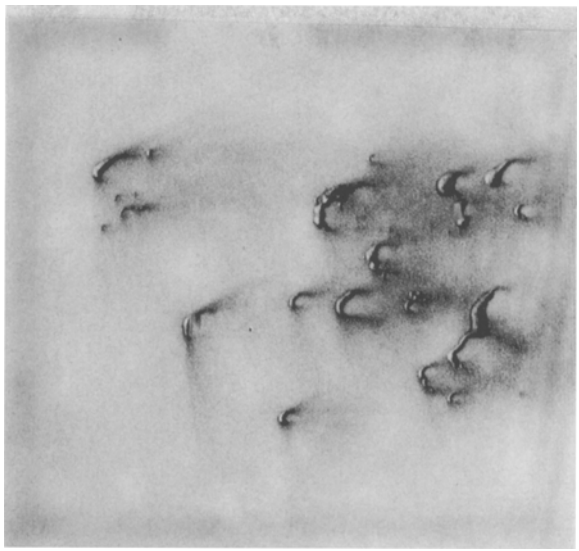

Fig. 5:

Barchan dunes of the martian north polar region; wind was blowing left to right when the dunes were active. Fine dark material emanating from the "horns" of the dunes suggested to Tsoar et al. (1979) that the dunes may be active; area shown is about 20 km by 20 km (Viking Orbiter image 544B05).

and on-pole winds that become westerly during winter. These wind patterns compare favorably with those based on models of the atmosphere (Pollack et al., 1990).

The low albedo (i.e., dark) of the north polar dunes suggests a composition other than quartz (the common sand composition on Earth), an observation fitting with the apparent lack of silicic materials on Mars (Krinsley et al., 1979). Because basaltic lavas are very common over much of Mars, including the smooth plains south of the dune field, one suggestion is that the north polar dunes are composed of windblown basaltic sand (Tsoar et al., 1979). Alternatively, studies of the colors of the dune deposits suggest that some of the material could be derived from the polar layered deposits (Thomas and Weitz 1989) or other local materials (Saunders and Blewett, 1987).

In addition to the north polar sand sea, dunes and dune fields are found in many places as isolated deposits (Fig. 4). Edgett and Christensen (1991, 1994) analyzed the thermal inertia properties of some of these deposits and estimated the particle sizes. They found an average size of 500 ± 100 μm, or medium to coarse sand, which is about twice the average size for dune deposits on Earth.

3.2. YARDANGS

Yardangs are wind-sculpted hills that have the appearance of inverted boat hulls. First discovered on Mariner 9 images (McCauley, 1973), most yardangs on Mars occur in equatorial regions, notably in the Amazonis region, Aeolis region, Ares Valles, and Iapygia. Some of the largest features are interpreted to be early-stage yardangs; they are 50 km long, 1 km wide, and 200 m high, and appear to have developed from the erosion of mesas. From studies of terrestrial yardangs, Ward (1979) concluded that the martian features are geologically young (on a martian time-scale) and probably are composed of friable rocks such as ignimibrites (many of the yardang localities are near known volcanic craters), or indurated regolith (regolith in this sense being fragmental debris

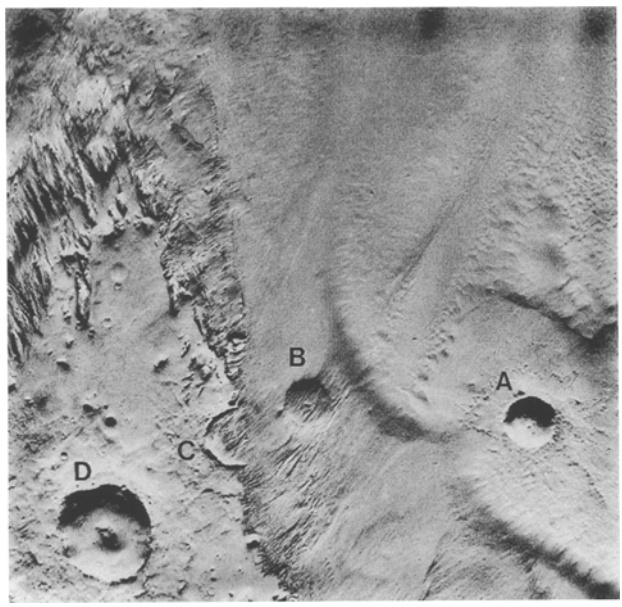

Fig. 6:
Exhumation of ancient cratered terrain (left side of image) as a younger mantling deposit (right side of image) is stripped away by the wind. Note the sequence of craters: A) fresh crater superposed on mantling deposit, B) mantled crater, C) half mantled, half exhumated crater, and D) exhumed crater. yardangs (wind-sculpted hills) form along the margins of the mantle; shown is about 75 km by 75 km (from Greeley et al., 1985) (Viking Orbiter image 438S01).

generated by impact cratering). On Earth yardangs develop by erosion of grains that are loosened by weathering processes involving liquid water; Ward suggests that on Mars (in the absence of liquid water) exfoliation, salt weathering, or freeze-thaw processes may operate, but that the net weathering rate would be slower than on Earth.

The orientations of the martian yardangs are inconsistent with wind directions predicted from global circulation model (GCM) runs simulating the atmosphere. This suggests that the yardangs formed under a different wind regime or that the yardang orientations are dominated more by structural patterns, such as joints or fractures, than by wind directions (Greeley et al., 1993).

Regardless of mode of formation or the material comprising the yardangs, the area containing the yardangs shown in Fig. 6 of the Amazonis region demonstrates the erosive potential by winds on Mars. This region originally consisted of ancient cratered terrain that was blanketed with mantling deposits of presumed windblown dust or volcanic ash. Subsequently, part of the cratered terrain has been exhumed, re-exposing the craters. The margins of the mantling blanket are being cut away by wind erosion, forming the yardangs.

3.3. VARIABLE FEATURES

Variable features were named from the Mariner 9 mission results (Sagan et al., 1972) for albedo patterns that changed their size, shape, and position with time. Crater streaks, the most common of the variable features, can occur as either light (Fig. 7) or dark forms, although 'mixed' forms are found in which both light and dark patterns occur in association with the same crater. Most investigators agree that streaks represent a

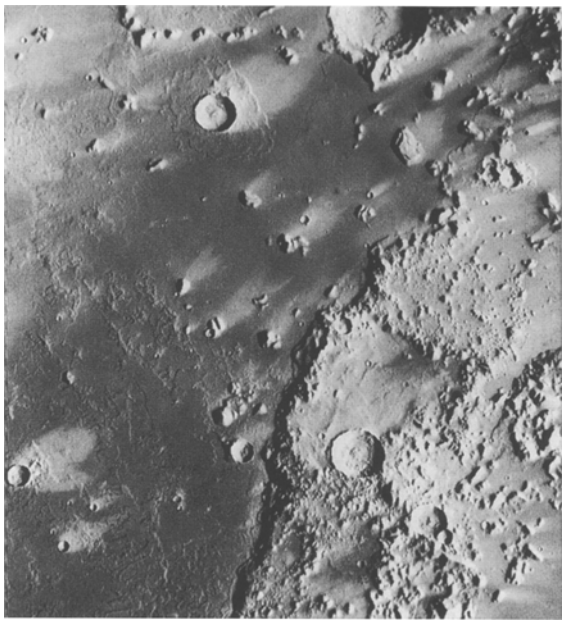

Fig. 7:
Bright wind streaks in the eastern Elysium Planitia region of Mars. Wind streaks are albedo patterns that have a contrast with the albedo of the surface on which they occur; note that the streaks in the lower right hand corner of the image are more difficult to discern because the background plains are also high albedo; area shown is about 150 km by 180 km (Viking Orbiter frame 545A54).

surface manifestation of windblown processes, such as relatively thin (~cm) deposits of particles that shift in response to winds.

Various models for streak formation have been proposed. Most models take into account the flow patterns generated by winds blowing over and around craters or other topographic features such as hills and ridges. Wind tunnel simulations and field studies show that a horseshoe vortex wraps around the crater rim and creates an erosive zone in the wake of the crater and a depositional zone in the immediate lee of the crater rim (Greeley et al., 1974). The size and shape of zones of erosion and deposition are functions of crater geometry, wind speeds, time, and other parameters (Iversen et al., 1976c). This model appears to be appropriate for explaining low albedo, or dark streaks. High albedo, or bright streaks appear to be dust deposits. Veverka et al. (1981) and Thomas et al. (1984) suggested that bright streaks form as a function of atmospheric stability, leading to dust deposition.

Crater streaks can be used to map surface wind patterns and be applied to atmospheric circulation models (Thomas and Veverka, 1979). A general circulation model (GCM) has been developed for Mars which enables near-surface wind direction and strength to be predicted as a function of season (Pollack et al., 1981, 1990). The model takes into account features such as dust opacity, surface albedo, and martian topography. Comparisons of wind streak locations and orientations visible on images provide a validation for the GCM and shed light on wind streak formation (Greeley et al., 1993). There is a good correlation between bright streaks and GCM predictions, both in terms of orientation and locations of maximum wind speeds during the southern hemisphere summer. Dark streaks, however, show poorer correspondence; this is

attributed to dark streak formation related to local winds that are not well represented by the GCM.

4. Venus

Aeolian processes on Venus have been debated for more than two decades, and many investigators predicted that aeolian features would eventually be found (reviewed by Greeley and Arvidson, 1990). Although images of the surface returned from the Soviet Venera landers and measurements of near-surface winds suggested local modification of the surface by wind, definitive evidence for more widespread aeolian activity was not observed until the Magellan mission (Saunders et al., 1991).

The atmosphere of Venus is composed primarily of CO_2 with minor amounts of hydrochloric, hydrofluoric, and sulfuric acids. With a surface pressure of more than 90 bar, it has the highest atmospheric density of all the terrestrial planets (Table 1). Venus is completely enveloped in a perpetual shroud of clouds that hide the surface from viewing. Repetitive pictures of the cloud tops obtained over a period of 8 days during the flyby of Mariner 10 in 1974 showed circulation patterns and allowed wind speeds to be determined for the upper atmosphere (Murray et al., 1974). From the cloud motion patterns, it was suggested that Hadley circulation dominated the upper atmosphere of Venus. Although speeds of about 100 m s^{-1} were obtained for the upper clouds in the equatorial zone, when extrapolations were made to the surface the winds were estimated to be very sluggish.

The Soviet landers, Venera 9 and 10, measured wind speeds near the surface for two sites on Venus of 0.5 to 1 m s^{-1} at the height of the windsensors (1 to 2 m above surface). More recent measurements of windspeeds obtained by the Pioneer-Venus atmospheric probes were extrapolated to the surface and yield values of 1 to 2 m s^{-1} (Counselman et al., 1979). These values are well within the range predicted for particle threshold (Fig. 1), based on a combination of theory (Hess, 1975; Sagan, 1975) and wind tunnel experiments (Iversen et al., 1976). Venera lander images of the surface show rock fragments several cm across and larger, set in a mass of fine (<1 cm) material interpreted to be sand size or smaller (Florensky et al., 1977). This bimodal size distribution is indicative of fluid transport and because liquid water cannot exist at the extremely high temperature on Venus, it is assumed that the fluid involved is the atmosphere, or wind.

Magellan synthetic aperture radar data reveal numerous surface features that are attributed to wind processes (Arvidson et al., 1991). These include dune fields, yardangs, and the most common aeolian feature, wind streaks (review by Greeley et al., 1994c).

4.1. WIND STREAKS

Venusian wind streaks are radar backscatter patterns that contrast with the surrounding surface (Arvidson et al., 1992; Greeley et al., 1992b). Both radar-bright (high radar backscatter, generally caused by rough surfaces) and radar-dark (low radar backscatter, generally resulting from smooth surfaces, or surfaces composed of particulate material such as sand) wind streaks occur. Although streaks range from less than 5 km long to several hundred kilometers, typical streaks are about 20 km long. Streaks occur in several shapes, including plume, fan, and long-narrow forms (Fig. 8). The most abundant, informally termed "zebra" streaks, consist of multiple, alternating radar dark and bright streaks. Nearly all zebra streaks are associated with deposits inferred to be

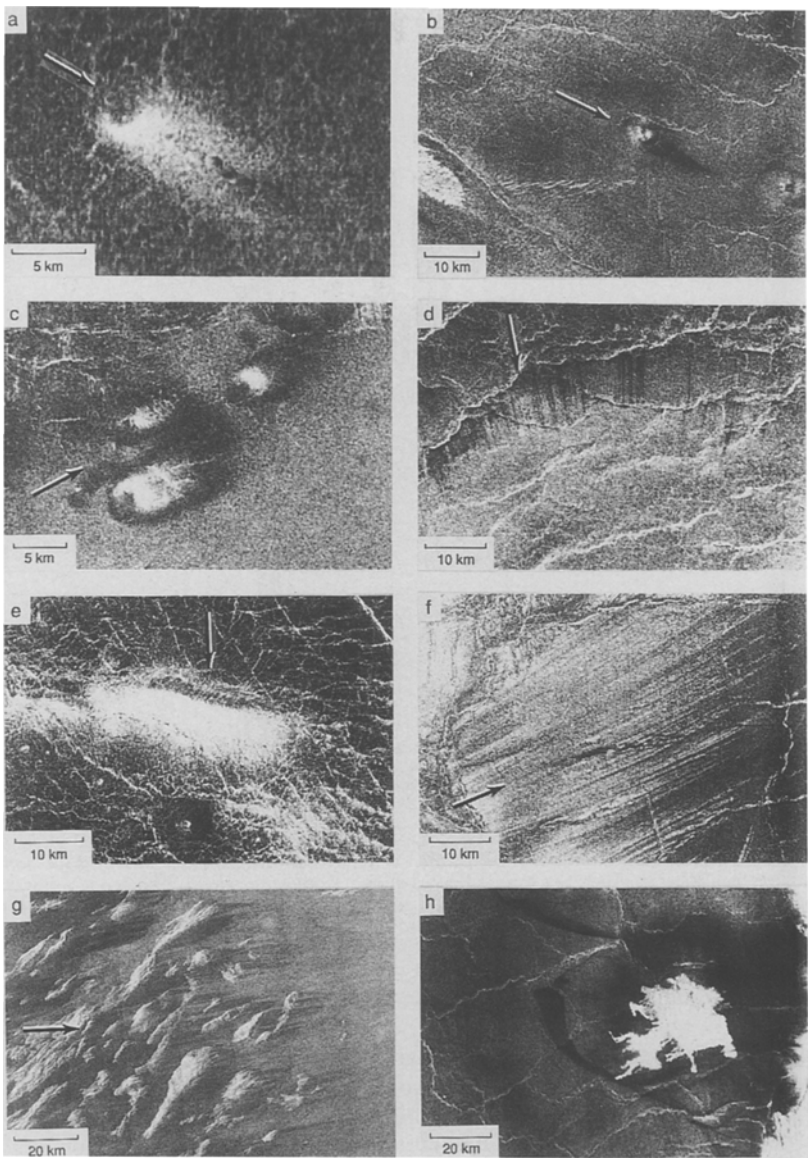

Fig. 8:

Venus wind streaks (arrows indicate downwind direction). (a) Radar-bright fan-shaped wind streak 10.5 km long associated with a small hill in eastern Niobe Planitia, centered at 36.5°N, 174.6°E (Magellan F-BIDR 1194). (b) Radar-dark fan-shaped wind streak about 10 km long associated with a small hill centered at 29.4°N, 57°E (Magellan MRPS 40983). (c) Radar-bright and -dark (mixed) fan-shaped wind streak in the Carson crater area, centered at 23°S, 344.9°E. Area shown is about 25 by 36 km (Magellan F-MIDR 23S345). (d) Linear wind streaks (radar-dark) associated with a ridge system in southern Leda Planitia, centered at 37.5°N, 65.5°E; area shown is about 44 by 64 km (Magellan MRPS 38883). (e) Transverse wind streak (radar-bright) associated with a ridge in Guinevere Planitia, centered at 26.2°N, 331.4°E; area shown is about 39 by 57 km (Magellan F-MIDR 25N333). (f) Multiple linear ("zebra") streaks in the vicinity of Mead crater, centered at 15°N, 65°E; area shown is about 44 by 64 km (Magellan MRPS 37877). (g) Multiple linear streaks (radar-dark) in western Aphrodite, centered at 0.9°S, 71.1°E; area shown is 82 by 120 km (Magellan F-MIDR 00N070). (h) Radar-dark wispy streak in eastern Sedna Planitia, centered at 37°N, 2°E; area shown is about 87 by 128 km (Magellan C1-MIDR 30N009) (from Greeley et al., 1992b).

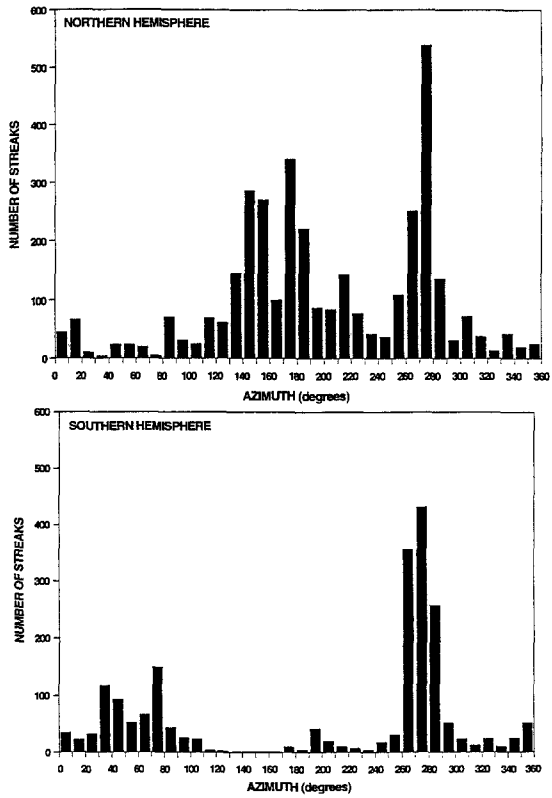

Fig. 9:
Histograms of wind streaks on Venus showing their azimuths (downwind orientation) for the northern and southern hemispheres. There is a bimodal distribution in both hemispheres. One mode is toward the equator, the other mode is toward the west. The equatorward component is consistent with Hadley circulation. The westward component is comprised of linear streaks associated with one class of venusian craters; the streaks are inferred to represent upper altitude westward zonal winds.

ejecta from young impact craters. More than 5970 wind streaks have been identified on Venus.

Similar to wind streaks on Earth and Mars (Sagan et al., 1972; Thomas et al., 1981; Greeley et al., 1989), venusian streaks are thought to be visible on radar images because of differences in the distribution of windblown particles as related to surface wind patterns. Wind tunnel experiments simulating Venus suggest that particles moved by the wind are smaller than ~1 cm, and that most would be a few hundred μm in diameter. Depending on the wind friction velocity, surfaces may be completely stripped of loose grains (leaving exposed bedrock), covered with large (>few cm) particles too massive to be removed by the wind (forming a lag deposit), or blanketed with grains transported from elsewhere and deposited in areas of low surface winds. Extremely rough surfaces, such as some lava flows, may serve as traps for wind-transported particles. Each of these surfaces would have different radar backscatter properties (Arvidson et al., 1992), depending on several considerations, including the areal extent and thickness of surficial deposits, exposed bedrock and its surface-roughness, and possible aeolian bedforms, such as dunes.

Most venusian wind streaks are associated with deposits from certain impact craters and some tectonically deformed terrains, suggesting that both of these geological

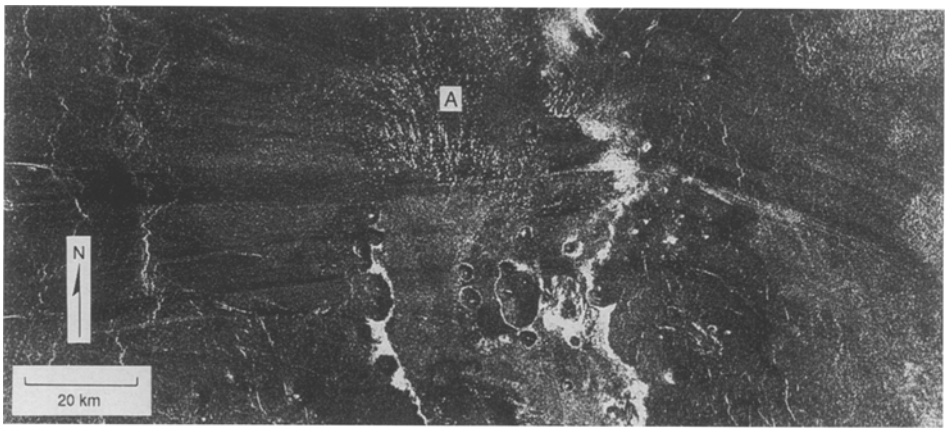

Fig. 10:
Aglaonice dune field, centered at 24.8°S; area shown is ~78 by 180 km. This dune field, indicated by the specular pattern at "A", is located with in outflow associated with the Aglaonice impact crater. Radar-dark linear streaks sweep across the area, suggesting winds from the east (right) toward the west (left). If this wind orientation is correct, the proposed dunes would be transverse forms (Magellan MRPS 34032); (from Greeley et al., 1992b).

settings provide fine particulate material that can be entrained by the low-velocity winds on Venus. Turbulence and wind patterns generated by the topographic features with which many streaks are associated can account for differences in particle distributions and in the patterns of the wind streaks. Thus, some high backscatter streaks are considered to be zones that are swept free of sedimentary particles to expose rough bedrock; other high backscatter streaks may be lag deposits of dense materials from which low-density grains have been removed (dense materials such as ilmenite or pyrite have dielectric properties that would produce high backscatter patterns).

To assess potential atmospheric circulation patterns on Venus, all wind streaks identified on Magellan images were mapped, measured, and classified (Greeley et al., 1994b). Histograms of streak orientations were plotted for the northern and southern hemispheres (Fig. 9). Orientations are given as azimuths in the downwind direction. In the northern hemisphere there is a bimodal distribution of azimuths; one mode is toward the south-southeast and the other is toward the west. The azimuths in the southern hemisphere are also bimodal with one mode toward the north-northeast and the second mode toward the west. Thus, the global wind directions inferred from the streaks are generally equatorward and toward the west.

Analysis of the orientations of venusian wind streaks suggests that the Hadley circulation proposed for the upper atmosphere extends to the surface, influencing the development of the streaks (Greeley et al., 1994b). Moreover, mapping the locations of the streaks suggests that Hadley cells extend to both polar areas of Venus.

4.2. OTHER AEOLIAN FEATURES

In addition to wind streaks, other aeolian features on Venus include yardangs (?) and dune fields. The Aglaonice dune field, centered at 25°S, 340°E, covers ~1290 km^2 and is located in an ejecta flow channel from the Aglaonice impact crater (Fig. 10). The Meshkenet dune field (Fig. 11), located at 67°N, 90°E, covers ~17,120 km^2 in a valley between Ishtar Terra and Meshkenet Tessera. Wind streaks associated with both dune fields suggest that the dunes are of transverse forms in which the dune crests are

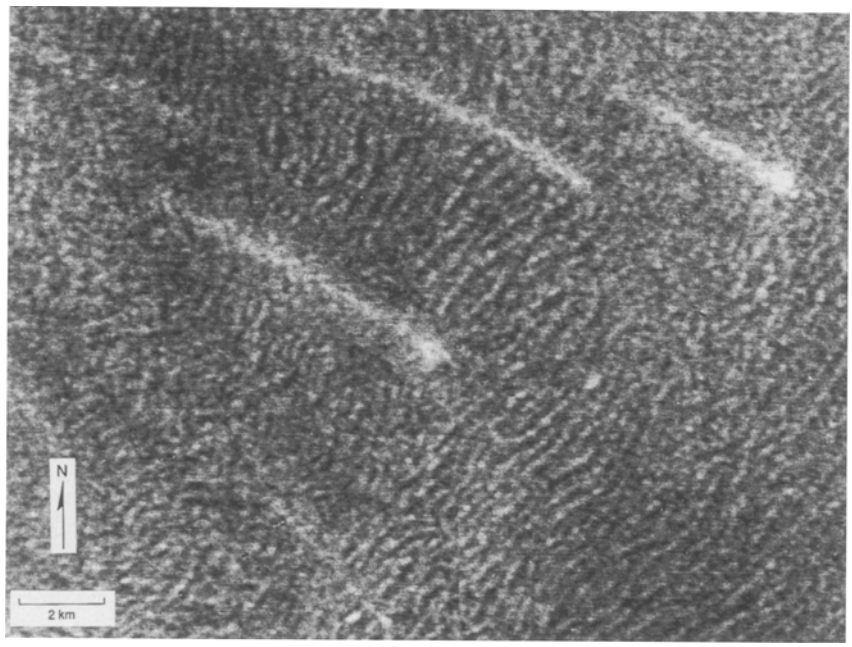

Fig. 11:
Part of the Fortuna-Meshkenet dune field (67.7°N, 90.5°E), showing transverse dunes and radar-bright wind streaks (Magellan MRPS 39824).

perpendicular to the prevailing winds. Dunes on Venus signal the presence of sand-size (~60 to 2,000 μm) grains.

The possible yardangs are found at 9°N, 60.5°E, about 300 km southeast of the crater Mead. The yardang field is in a slight topographic depression between a ridged belt to the northwest and the flank of Aphrodite Terra to the southeast. Analysis of fan-shaped wind streaks suggests that winds are "funneled" through the depression toward the equator. The orientations of the yardangs are consistent with this flow pattern, suggesting that the yardangs were eroded by the same wind regime which formed the fan-shaped streaks.

Wind streaks and dune fields were examined on both Magellan Cycle-1 and Cycle-2 SAR images to determine if any changes had taken place in the 8-month interval between the two sequences. No changes could be detected that could be attributed definitively to aeolian processes. However, as noted by Weitz et al. (1994), bright and dark patches in several regions of the southern hemisphere were found to be visible on SAR images of one cycle, but not the other. These patches are suggested to be zones of microdunes in which the steeper, slip face produced a higher backscatter return when viewed from one direction (i.e., one cycle) but when viewed from the opposite direction (i.e., opposing cycle), the gentle, windward face produced little backscatter.

Microdunes were first proposed on Venus from analysis of Venera images (Florensky et al., 1977). Wind tunnel simulations under venusian conditions generated microdunes of 10-15 cm wavelength and a few cm high which had all the characteristics of full-scale dunes, including internal bedding structures. Weitz et al. (1994) suggested that the size and geometry are appropriate for the detection of microdunes on Magellan images as a function of "look" direction.

5. Summary and conclusions

Terrestrial planets that have dynamic atmospheres are Earth, Mars, and Venus. Depending on environments, these planets experience a variety of surface-modifying processes including weathering, erosion, and deposition. Winds currently shape all three planets and geological evidence shows that aeolian processes have operated throughout their "visible" history.

Wind erosional landforms (yardangs, eroded rocks, deflation pits), depositional landforms (dunes, mantling deposits), and wind streaks are seen on Earth, Mars, and Venus. Determining the location and age of these features gives insight into geologic histories and the interactions of the atmosphere and the surface.

Some of the key problems to be addressed for Mars and Venus in the future include:

- Determining the particle size and geographic distribution of windblown materials,
- Determining if and how cycles of windblown materials operate,
- Determining if sand dunes are currently active,
- Determining rates of erosion and deposition,
- Determining the composition(s) of windblown material,
- Determining the time scales of wind streak evolution.

Some of these issues will be addressed for Mars on forthcoming missions such as Mars Global Surveyor, Mars Pathfinder, and Mars-96. With no currently approved missions for Venus, many of these issues will not be addressed for years; however, the Magellan data set undoubtedly has much to yield with further analysis.

References

Arvidson, R.E., Binder, A.B., and Jones, K.L. (1978) The surface of Mars, *Sci. Amer.* **128**, No. 3, 76-89.

Arvidson, R.E., Baker, V.R., Elachi, C., Saunders, R.S., and Wood, J.A. (1991) Magellan analysis of Venus surface modification, *Science* **252**, 270-275.

Arvidson, R.E., Greeley, R., Malin, M., Saunders, R.S., Izenberg, N., Plaut, J.J. and Stofan, E. (1992) Surface modification of venus as inferred from Magellan observations of plains and tesserae, *J. Geophys. Res.* **97**, 13,303-13,317.

Bagnold, R.A. (1941) *The Physics of Blown Sand and Desert Dunes*, Methuen and Co., London, 265 p.

Breed, C.S., Grolier, M.J., and McCauley, J.F. (1979) Morphology and distribution on common 'sand' dunes on Mars: Comparison with Earth. *J. Geophys. Res.* **84**, 8183-8204.

Briggs, G., Klaasen, K. Thorpe, T., and Wellman, J. (1977) Martian dynamical phenomena during June-November 1976: Viking Orbiter imaging results. *J. Geophys. Res.* **82**, 4121-4149.

Christensen, P.R. (1986) Regional dust deposits on Mars: Physical properties, age, and history, *J. Geophys. Res.* **91**, 3533-3545.

Christensen, P.R. (1988) Global albedo variations on Mars: Implictions for active aeolian transport, deposition, and erosion, *J. Geophys. Res.* **93**, 7611-7624.

Christensen, P.R. and Moore, H.J. (1992) The Martian surface layer, in H.H. Kieffer, B.M. Jakosky, C.W. Snyder, and M.S. Matthews (eds.), *Mars*, Univ. of Arizona Press, Tucson, pp. 686-729.

Counselman, C.C., Gourevitch, S.A., King, R.W., Loriot, G.B., and Prinn, R.G. (1979) Venus winds and zonal and retrograde below the clouds, *Science* **205**, 85-87.

Cutts, J.A. and. Smith, R.S.U (1973) Eolian deposits and dunes on Mars, *J. Geophys. Res.* **78**, 4139-4154.

Edgett, K.S. and Christensen, P.R. (1991) The particle size of Martian aerolian dunes, *J. Geophys. Res.* **96**, 22,765-22,776.

Edgett, K.S. and Christensen, P.R. (1994) Mars aeolian sand: Regional variations among dark-hued crater floor features, *J. Geophys. Res.* **99**, 1997-2018.

Florensky, C.P., Ronca, L.B., Basilevsky, A.T., Burba, G.A., Nikolaeva, O.V., Pronin, A.A., Trakhtman, A.M., Volkov, V.P., and Zazetsky, V.V. (1977) The surface of Venus as revealed by Soviet Venera 9 and 10, *Geol. Soc. of Amer. Bull.* **88**, 1537-1545.

Greeley, R. and Arvidson, R.E. (1990) Aeolian processes on Venus. *Earth, Moon, and Planets 50/51*, pp. 127-157.

Greeley, R. and Iversen, J.D. (1985) *Wind as a Geological Process*, University of Cambridge Press, Cambridge, 333 p.

Greeley, R., Iversen, J.D., Pollack, J.B., Udovich, N., and White, B. (1974) Wind tunnel simulations of light and dark streaks on Mars, *Science* **183**, 847-849.

Greeley, R., White B., Leach, R., Iversen, J., and Pollack, J. (1976) Mars: wind friction speeds for particle movement, *Geophys. Res. Let.* **3**, 417-420.
Greeley, R., White, B.R., Pollack, J.B., Iversen, J.D., and Leach, R.N. (1977) Dust storms on Mars: Considerations and simulations. *NASA Tech. Memo, TM 78423,* 29 p.
Greeley, R., Leach, R., White, B., Iversen, J., and Pollack, J. (1980) Threshold windspeeds for sand on Mars: Wind tunnel simulations, *Geophys. Res. Let.* **7**, 121-124.
Greeley, R., Williams, S.H., White, B.R., Pollack, J.B., and Marshall, J.R. (1985) Wind abrasion on Earth and Mars, in M.J. Woldenberg (ed.), *Models in Geomorphology*, Allen & Unwin, Boston, pp. 373-422.
Greeley, R., Christensen, P., and Carrasco, R. (1989) Shuttle radar images of wind streaks in the Altiplano, Bolivia, *Geology* **17**, 665-668.
Greeley, R., Lancaster, N., Lee, S., and Thomas, P. (1992a) Martian aeolian processes, sediments, and features, in H.H. Kieffer, B.M. Jakosky, C.W. Snyder and M.S. Matthews (Eds.), *Mars*, Univ. of Arizona Press, Tucson, pp. 730-766.
Greeley, R., Arvidson, R.E., Elachi, C., Geringer, M.A., Plaut, J.J., Saunders, R.S., Schubert, G., Stofan, E.R., Thouvenot, E.J.P., Wall, S.D., and Weitz, C.M. (1992b,) Aeolian features on Venus: Preliminary Magellan results, *J. Geophys. Res.* **97**, 13,319-13,345.
Greeley, R., Skypeck, A., and Pollack, J.B. (1993) Martian aeolian features and deposits: Comparisons with general circulation model results, *J. Geophys. Res.* **98**, 3183-3196.
Greeley, R., Lacchia, M., White, B.R., Leach, R, Trilling, D., and Pollack, J. (1994a) Dust on Mars: New values for wind threshold, *Lunar and Planetary Science* **25**, 467-468.
Greeley, R., Schubert, G., Limonadi, D., Bender, K.C., Newman, W.I., Thomas, P.E., Weitz, C.M., and Wall, S.D. (1994b) Wind streaks on Venus: Clues to atmospheric circulation, *Science* **263**, 358-361.
Greeley, R., Bender, K., Thomas, P.E., Schubert, G., Limonadi, D., and Weitz, C.M. (1994c) Wind related features and processes on Venus: Summary of Magellan results, *Icarus* (submitted).
Hess, S.L. (1975) Dust on Venus, *J. Atmos. Sci.* **32**, 1076-1078.
Iversen, J.D., Greeley, R. and Pollack, J.B. (1976a) Windblown dust on Earth, Mars and Venus, *J. Atmos. Sci.* **33**, 2425-2429.
Iversen, J.D., Pollack, J.B., Greeley, R., and White, B.R. (1976b) Saltation threshold on Mars: The effect of interparticle force, surface roughness, and low atmospheric density, *Icarus* **29**, 381-393.
Iversen, J.D., Greeley, R., White B.R., and Pollack, J.B. (1976c) The effect of vertical distortion in the modeling of sedimentation phenomena: Martian crater wake streaks, *J. Geophys. Res.* **81**, 4846-4856.
Kahn, R.A., Martin, T.Z., Zurek, R.W. and Lee, S.W. (1992) The Martian dust cycle, in H.H. Kieffer, B.M. Jakosky, C.W. Snyder and M.S. Matthews (eds.), *Mars*, Univ. of Arizona Press, Tucson, pp. 1017-1053.
Krinsley, D.H., Greeley, R., and Pollack, J.B. (1979) Abrasion of windblown particles on Mars--erosion of quartz and basaltic sand under simulated martian conditions, *Icarus* **39**, 364-84.
Lee, S.W., Thomas, P.C., and Veverka, J. (1982) Wind streaks in Tharsis and Elysium: Implications for sediment transport by slope winds, *J. Geophys. Res.* **87**, 10025-10042.
Martin, L.J. and Zurek, R.W. (1993) An analysis of the history of dust activity on Mars, *J. Geophys. Res.* **98**,3221-3246.
McCauley, J.F. (1973) Mariner 9 evidence for wind erosion in the equatorial and mid-latitude regions of Mars, *J. Geophys. Res.* **78**, 4123-4137.
Murray, B.C., Belton, M.J.S., Danielson, G.E., Davies, M.E., Gault, D., Hapke, B., O'Leary, B., Strom, R.G., Soumi, V., and Trask, N. (1974) Venus: Atmospheric motion and structure from Mariner 10 pictures, *Science* **183**, 21-29.
Pollack, J.B., Leovy, C.B., Greiman, P.W., and Mintz, Y. (1981) A martian general circulation experiment with large topography, *J. Atmos. Sci.* **38**, 3-29.
Pollack, J.B., Haberle, R.M., Schaeffer, J., and Lee, H. (1990) Simulations of the general circulation of the martian atmosphere 1: Polar processes, *J. Geophys. Res.* **95**, 1447-1473.
Sagan, C. (1975) Windblown dust on Venus, *J. Atmos. Sci.* **32**, 1079-1083.
Sagan, C. and Pollack, J.B. (1969) Windblown dust on Mars, *Nature* **223**, 791-794.
Sagan, C., Veverka, J., Fox, P., Dubisch, R., Lederberg, J., Levinthal, E., Quam, L., Tucker, R., Pollack, J.B., and Smith, B.A. (1972) Variable features on Mars: Preliminary Mariner 9 television results, *Icarus* **17**, 346-372.
Saunders, R.S. and Blewett, D.T. (1987) Mars north polar dunes: Possible formation from low-density sediment aggregates, *Astronomical Vestn.* **21**, 181-188.
Saunders, R.S., Arvidson, R.E., Head, J.W. III, Schaber, G.G., Stofan, E.R., and Solomon, S.C. (1991) An overview of Venus geology, *Science* **252**, 249-252.
Thomas, P. and Gierasch, P.J. (1985) Dust devils on Mars, *Science* **230**, 175-177.
Thomas, P. and Weitz, C. (1989) Sand dune materials and polar layered deposits on Mars, *Icarus* **81**, 85-215.
Thomas, P., Veverka, J., Lee, S., and Bloom, A (1981) Classification of wind streaks on Mars, *Icarus* **45**, 124-153.
Thomas, P. Veverka, J., Gineris, D., and Wong, L. (1984) "Dust" streaks on Mars, *Icarus* **60**, 161-179.
Tsoar, H., Greeley, R., and Peterfreund, A.R. (1979) Mars: The north polar sand sea and related wind patterns, *J. Geophys. Res.* **84**, 8167-8180.
Veverka, J., Gierasch, P., and Thomas, P. (1981) Wind streaks on Mars: Meteorological control of occurrence and mode of formation, *Icarus* **45**, 154-166.
Ward, A.W. (1979) Yardangs on Mars: evidence of recent wind erosion, *J. Geophys. Res.* **84**, 8147-8166.
Weitz, C.M., Plaut, J.J., Greeley, R., and Saunders, R.S. Dunes and microdunes on Venus: Why were so few found in the Magellan Data?, *Icarus*, in press.

Zurek, R.W., Barnes, J.R., Haberle, R.M., Pollack, J.B., Tillman, J.E., and Leovy, C.B. (1992) Dynamics of the atmosphere of Mars, in H.H. Kieffer, B.M. Jakosky, C.W. Snyder and M.S. Matthews (eds.), *Mars*, Univ. of Arizona Press, Tucson, pp. 835-933.